Available online at www.sciencedirect.com
SCIENCE DIRECT®
Polyhedron 24 (2005) 731–738
POLYHEDRON
www.elsevier.com/locate/poly

Synthesis, properties and gas phase collision-induced dissociation of the heptanuclear doubly bridged complex $[Ru(bpy)_2(BPE)_2\{Ru_3O(CH_3COO)_6(py)_2\}_2](PF_6)_4$

Henrique E. Toma [a,*], Sofia Nikolaou [b], Marcos N. Eberlin [c], Daniela M. Tomazela [c]

[a] *Instituto de Química, Universidade de São Paulo, CaixaPostal 26077, CEP 05513-970, São Paulo, Brazil*
[b] *Departamento de Química, Faculdade de Filosofia, Ciências e Letras de Ribeirão Preto, Universidade de São Paulo, FFCLRP – USP, Ribeirão Preto, Brazil*
[c] *Instituto de Química, Laboratório Thomson de Espectrometria de Massas, Universidade Estadual de Campinas UNICAMP, Campinas, Brazil*

Received 30 June 2004; accepted 27 January 2005
Available online 25 March 2005

Abstract

The $[Ru(bpy)_2(BPE)_2\{Ru_3O(CH_3COO)_6(py)_2\}_2](PF_6)_4$ complex, in which bpy = 2,2′-bipyridine, BPE = *trans*-1,2-*bis*(4-pyridyl)ethylene and py = pyridine, provides an interesting case of a heptanuclear mixed compound containing two triangular $[Ru_3O]$ clusters attached to a ruthenium polypyridine center. The composition and structural properties of this doubly bridged complex were investigated by means of electrospray mass (ESI-MS) and tandem mass (ESI-MS/MS) spectrometric experiments and NMR spectroscopy (^1H and ^{13}C). The characteristic multi-isotopic distribution, 1/4 *m*/*z* peak separation and dissociation chemistry of the isotopologue $[Ru(bpy)_2(BPE)_2\{Ru_3O(CH_3COO)_6(py)_2\}_2]^{4+}$ cation provided detailed and unequivocal MS characterization of the complex. In the electronic spectra of the heptanuclear complex broad bands were observed at 427 and 696 nm, and ascribed, respectively, to $[Ru(bpy)_2(BPE)_2]$ metal-to-ligand charge-transfer and to $[Ru_3O]$ internal cluster transitions. The characteristic waves associated with the $[Ru_3O]^{1-/0/1+/2+/3+}$ redox couples were found at −1.02, 0.16, 1.20, 2.11 V (versus SHE) in the cyclic voltammograms. Another broad wave was observed at −1.22 V, involving superimposed $bpy^{0/-}$ and $BPE^{0/1-}$ redox processes, and a peculiar wave at 1.48 V, exhibiting only a half of the relative intensity, was assigned to the central $Ru^{3+/2+}$ redox pair. Despite the two conjugated BPE bridges, the electrochemical and spectroelectrochemical data indicated only a weak coupling through the π-system in the heptanuclear complex.

Keywords: Ruthenium clusters; Ruthenium polypyridines; Polynuclear complexes; ESI-MS

1. Introduction

Trinuclear complexes of the general formula $[M_3O(CH_3COO)_6(L)_3]^n$ (M = transition metal, L = solvent or *N*-heterocyclic ligands) feature a triangular structure in which the metal ions are held together by μ-oxo and carboxylate bridges [1–3]. In the particular case of triruthenium compounds, the electronic interaction among the ruthenium ions is usually so strong that the central core $[Ru_3O]^+$ is totally delocalized, behaving as a single metal center [1–4]. From an electrochemical viewpoint, it constitutes an appealing electroactive moiety, since the $[Ru_3O]$ unit displays up to five reversible redox processes in the −1.5 to 2.5 V (versus SHE) range and the choice of terminal and bridging ligand modulates its electrochemical behavior [5,6]. Moreover, each monoelectronic process is accompanied by drastic

* Corresponding author. Tel.: +55 11 30913887; fax: +55 11 38155579.
E-mail address: henetoma@iq.usp.br (H.E. Toma).

0277-5387/$ - see front matter © 2005 Elsevier Ltd. All rights reserved.
doi:10.1016/j.poly.2005.01.020

chromatic changes [7,8] providing a suitable combination of electronic stimuli and spectroscopic response.

More recently, these trinuclear ruthenium complexes have been increasingly used in the assembly of supramolecular structures [9–11] and to study intramolecular electron transfer reactions in symmetric dimers [12]. The binding of these species to ruthenium polypyridines complexes, simulating $[Ru(bpy)_3]^{2+}$ [13–16], would provide interesting prototypes to study photoinduced energy or electron transfer reactions.

The *trans*-1,2-*bis*(4-pyridyl)ethylene bridge (BPE) is also of interest as such a species belongs to a class of organic ligands bearing C=C double bonds capable of undergoing reversible *trans* → *cis* photoisomerization [17–19]. This type of functionality is being currently exploited for storage and processing information at the molecular level. The isomerization driven by light can actually lead to selective changes in the molecular conformation, modifying the spectroscopic behavior of the system in a controllable fashion [20,21] and promoting, in some cases, molecular motion [22].

This work deals with the chemistry of the BPE doubly bridged heptanuclear complex $[Ru(bpy)_2(BPE)_2\{Ru_3O(CH_3COO)_6(py)_2\}_2](PF_6)_4$ (Fig. 1). We report herein a unique assembly of polymetallic species that combines the rich redox characteristics of the cluster species and the remarkable chemical and photophysical properties of ruthenium(II) polypyridine complexes. Special emphasis is given to its structural characterization by means of NMR spectroscopy (^1H and ^{13}C), and electrospray mass (ESI-MS) and tandem mass (ESI-MS/MS) spectrometric experiments. The MS experiments, in particular, confirms the characteristic multi-isotopic distribution and dissociation chemistry expected for a $[Ru(bpy)_2(BPE)_2\{Ru_3O(CH_3COO)_6(py)_2\}_2]^{4+}$ quadruply charged gaseous cation providing detailed and unequivocal MS characterization of this heptanuclear doubly bridged ruthenium complex.

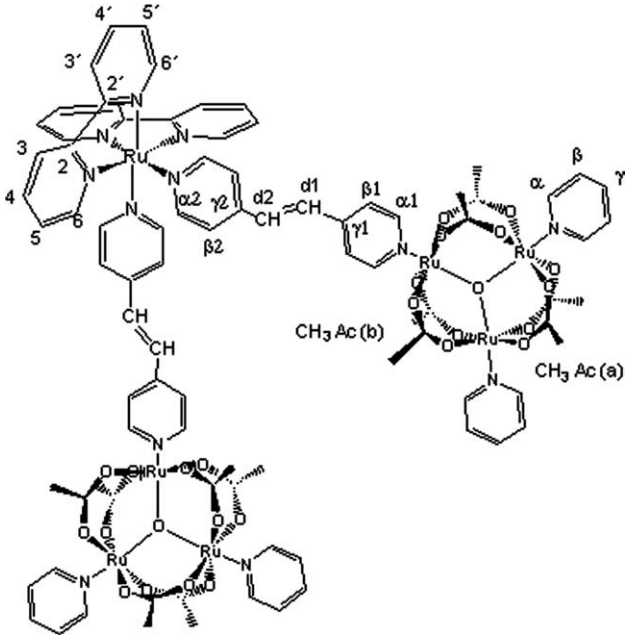

Fig. 1. Structural representation of the heptanuclear complex $[Ru(bpy)_2(BPE)_2\{Ru_3O(CH_3COO)_6(py)_2\}_2]^{4+}$ in which the numbering scheme for the assignment of the corresponding NMR spectra is also indicated.

2. Experimental

2.1. Synthesis

The $[Ru(bpy)(BPE)_2](PF_6)_2$ and $[Ru_3O(CH_3COO)_6(py)_2(CH_3OH)]PF_6$ complexes were synthesized according to reported procedures [10,23].

2.1.1. $[Ru(bpy)_2(BPE)_2\{Ru_3O(CH_3COO)_6(py)_2\}_2](PF_6)_4$

$[Ru(bpy)_2(BPE)_2](PF_6)_2 \cdot 2H_2O$ (60 mg, 0.056 mmol) was dissolved in CH_2Cl_2 (20 ml) and allowed to react with $[Ru_3O(CH_3COO)_6(py)_2(CH_3OH)]PF_6$ (113 mg, 0.112 mmol) for 72 h, at room temperature, in the dark. The solution was filtered and the liquid was treated with diethyl ether, giving a greenish brown solid. This material was collected on a filter, dissolved in CH_2Cl_2 and purified by chromatography using a neutral alumina column. The product was eluted with a mixture of 50% CH_3CN:CH_2Cl_2 (v/v) and the corresponding solution was evaporated to dryness. After dissolving in a minimum volume of CH_2Cl_2, the solution was filtered onto stirring diethyl ether, giving a dark solid, which was collected on a filter and washed with diethyl ether (50 mg, 30%). Required for $C_{88}H_{92}N_{12}O_{26}Ru_7P_4F_{24} \cdot 3(C_4H_{10}O)$: C, 37.0; H, 3.8; N, 5.2. Found: C, 37.4; H, 4.1; N, 5.6%.

2.2. Physical measurements

Electrospray ionization mass and tandem mass spectra were recorded on a Q-Tof (Micromass) mass spectrometer with quadrupole (Qq) and high resolution orthogonal time of flight (o-TOF) hybrid configuration operated under conditions described in detail elsewhere [24]. The sample introduction was performed using a syringe pump (Harvard Apparatus, Pump 11) set to 10 μl/min pumped through an uncoated fused-silica capillary. All samples were dissolved in pure methanol. The ESI mass spectrum was acquired using an ESI capillary voltage of 3 kV and a cone voltage of 10 V. For the ESI tandem mass spectrum, the mass-selected ions were dissociated using 20 eV collisions with argon.

One dimensional ^1H NMR spectra and two dimensional COSY and HETCOR spectra were recorded on a Varian 300 MHz, model INOVA 1 spectrometer, employing 2×10^{-2} mol l CD_3CN solutions, at room

temperature. UV–Vis spectra were recorded on a Hewlett-Packard model 8453 diode array spectrophotometer, using 10^{-5} mol l solutions.

Cyclic voltammetry was carried out with a Princeton Applied Research model 283 potentiostat. A platinum disk electrode was employed for the measurements, using the conventional Luggin capillary arrangement with an $Ag/AgNO_3$ (0.010 mol l) reference electrode in CH_3CN containing 0.100 mol l tetraethylammonium perchlorate (TEAP). A platinum wire was used as the auxiliary electrode. All the $E_{1/2}$ values presented here were converted to SHE by adding 0.503 V to the observed values. A three electrode system was used for the spectroelectrochemical measurements, arranged in a rectangular quartz cell of 0.025 cm internal optical path length. A gold minigrid was used as transprecursor working electrode, in the presence of the above mentioned auxiliary and reference electrodes.

Steady-state emission spectra were recorded on a LS-100 Photon Technology International Inc. spectrophotometer, at room temperature and 77 K. Photoisomerization measurements were carried out with a 150 W Xenon Arc Lamp and a f/3.4 Monochromator (Applied Photophysics), by irradiating 10% CH_3CN:H_2O samples of the BPE ligand at 313 nm and of the heptanuclear species at 297 nm.

3. Results and discussion

3.1. ^1H and ^{13}C NMR spectra

The ^1H and ^{13}C NMR spectra of the $[Ru(bpy)_2(BPE)_2\{Ru_3O(CH_3COO)_6(py)_2\}_2](PF_6)_4$ complex are complicated by the large number of signals. Preliminary analysis indicated five non-magnetically equivalent types of aromatic rings: the pyridine rings, two peripheral bpy rings (labelled as **2**, **3**, **4**, **5**, **6** and **2′**, **3′**, **4′**, **5′**, **6′**) and two different rings corresponding to the bridging ligand, one bound to the $[Ru_3O]$ core and the other bound to the $[Ru(bpy)_2]$ center. The assignment was made based on careful evaluation of the 2D correlation NMR spectra, guided by a comparison with data for the complex $[Ru_3O(CH_3COO)_6(py)_2(BPE)]PF_6$ and with the literature data [25,26].

As one can see in Table 1, the δ values of the $[Ru(bpy)_2]$ protons follow the same trends observed for the $[Ru(bpy)_3]^{2+}$ complex [25,27]; the same behavior is observed for the ^{13}C signals in comparison with the free bpy ligand. Owing to coordination to the ruthenium ion, free rotation of the bpy rings is not possible; hence protons **3** and **3′** are sterically strained in such a way that the Van der Waals interaction between them causes a deshielding effect, shifting their signals to lower field in relation to other protons of that ligand. As expected, protons **4**, **5** and **5′** appear as triplets with values of δ varying between 7.2 and 8.1 ppm due to the non-equivalence of the bpy rings. Protons **4′** are superimposed with protons **6′**.

Table 1
^1H and ^{13}C chemical shifts (δ/ppm) for the heptanuclear complex $[Ru(bpy)_2(BPE)_2\{Ru_3O(CH_3COO)_6(py)_2\}_2](PF_6)_4$ in CD_3CN solution (see labels in Fig. 1)

Position	(^1H) δ/ppm		(^{13}C) δ/ppm	
	Complex	Free ligand[a]	Complex	Free ligand[a]
Pyridine				
α	0.17	8.6	126.61	149.9
β	5.80	7.2	115.13	123.7
γ	6.56	7.6	138.64	135.7
Acetate				
CH_3 (a)	4.88	2.1	−4.10	20.7
CH_3 (b)	4.78	2.1	−4.10	20.7
C═O (a), (b)			200.16	177.7
BPE				
α_1	0.47	8.65	126.47	150.7
β_1	6.06	7.45	112.75	121.4
γ_1, γ_2			145.35	145.5
d_1	6.71	7.29	129.60	130.5
d_2	~7.14[b]	7.29	131.32	130.5
β_2	~7.14[b]	7.45	124.20	121.4
α_2	8.14	8.65	158.48	150.7
2,2′-Bipyridine				
2,2′			154.76	156.2
3′	8.24	8.42	124.74	123.5
3	8.31	8.42	125.04	123.5
4′	7.83	7.77	138.93	136.7
4	8.02	7.77	139.03	136.7
5′	7.28	7.25	128.58	121.0
5	7.66	7.25	128.95	121.0
6′	7.79	8.67	153.42	149.1
6	8.79	8.67	153.60	149.1

[a] Data from Ref. [30].
[b] H signals d_2 and β_2 are superimposed.

Protons **6′** are subjected to the so called *ring current* effects. These protons are located in the shielding region of the pyridinic aromatic rings and, therefore, have their signals shifted to higher field in relation to the free ligand. However, protons **6** appear downfield shifted; this shift could be addressed assuming that the BPE rings are not co-planar to each other, being otherwise inclined in such a way that subjects protons **6** to the deshielding region.

For the $[Ru_3O(CH_3COO)_6(py)_2]$ moiety, the δ values (Table 1) follow the pattern dictated by the paramagnetic anisotropy of the $[Ru_3O]$ core [1].

In the heptanuclear complex, two signals assigned to the acetate protons are observed (consistent with the presence of two magnetically non-equivalent acetate sites; i.e., four *vicinal* and two in opposite positions with respect to the bridging ligand). For the BPE bridging ligand, a splitting in the proton (and carbon) signals (Table 1) is observed, attributed to the double bond, which constitute a singlet in the free ligand. This split-

ting reflects a decrease in the symmetry of the ligand owing to the bridging coordination mode between two different metallic units. Note that the J coupling constant of the d_1 proton is equal to 16.5 Hz, a value that is typical for the *trans*-isomer [28]. This signal is shifted to higher field, showing that it is sensitive to the paramagnetic anisotropy of the [Ru_3O] unit. This effect is also expressed in the δ values observed for the α_1 and β_1 protons attached to the BPE ring directly bound to the paramagnetic center and for the pyridinic rings, whose corresponding protons appear shifted to higher fields in relation to free pyridine. The magnitude of this effect diminishes with the distance from the [Ru_3O] core and this pattern can be explained considering both dipolar and contact mechanisms for the paramagnetic interactions in the molecule [29]. These interactions are also responsible for the fact that the signals for the acetate methyl protons are shifted in the opposite direction as those of pyridine, whereas inverse trends for protons and carbon shifts are observed for the acetate signals.

3.2. Mass spectrometric structural characterization

ESI-MS and ESI-MS/MS experiments are being increasingly used in the structural characterization of organometallic and metallorganic species, as well as of loosely bonded cationic and ionic coordination species participating as key reaction intermediates [31,32]. In our case, ESI provided an efficient technique for "fishing" directly from solution to the gas phase, both ionic components of the supramolecular complex [Ru(bpy)$_2$(BPE)$_2${Ru$_3$O(CH$_3$COO)$_6$(py)$_2$}$_2$](PF$_6$)$_4$, i.e., either the quadruply charged cationic species [Ru(bpy)$_2$(BPE)$_2${Ru$_3$O(CH$_3$COO)$_6$(py)$_2$}$_2$]$^{4+}$ or the singly charged anionic species PF_6^-, allowing their corresponding mass detection, and isotopic and structural characterization.

The ESI mass spectrum in the positive ion mode of a methanolic solution of the complex detected a prominent cluster of isotopologue cations (*m*/*z* 610 for the most abundant) separated by 1/4 *m*/*z* units, which matched perfectly the features expected for Ru(bpy)$_2$(BPE)$_2${Ru$_3$O(CH$_3$COO)$_6$(py)$_2$}$_2$]$^{4+}$. The characteristic, multi-component isotopic pattern resulting from the presence of seven multi-isotope ruthenium atoms also matched perfectly that calculated for this cation. The ESI mass spectrum in the negative ion mode detected a prominent single and monoisotopic anion of *m*/*z* 145 (144.96) corresponding to PF_6^-.

For structural characterization, the entire cluster of the many quadruply charged isotopologue ions [Ru(bpy)$_2$(BPE)$_2${Ru$_3$O(CH$_3$COO)$_6$(py)$_2$}$_2$]$^{4+}$ (*m*/*z* 610) were mass-selected and subjected to 15 eV collision-induced dissociation (Fig. 2). Dissociation was observed to occur mainly by successive breaking of the BPE–ruthenium bonds, showing this bond to be the weakest for the complex. As summarized in Fig. 3, the quadruply

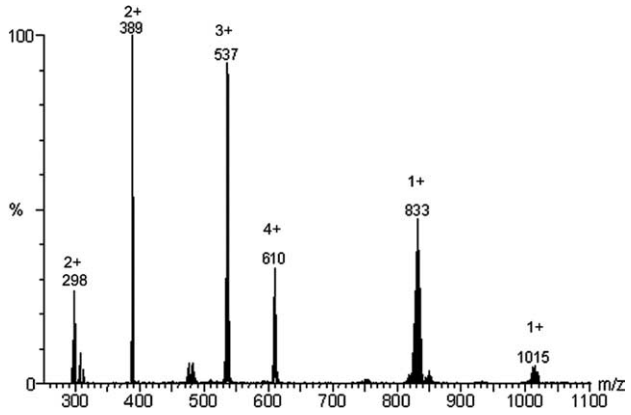

Fig. 2. ESI tandem mass spectrum for 15 eV collision-induced dissociation of [Ru(bpy)$_2$(BPE)$_2${Ru$_3$O(CH$_3$COO)$_6$(py)$_2$}$_2$]$^{4+}$ ions (*m*/*z* 610). The charge states for the ions are indicated.

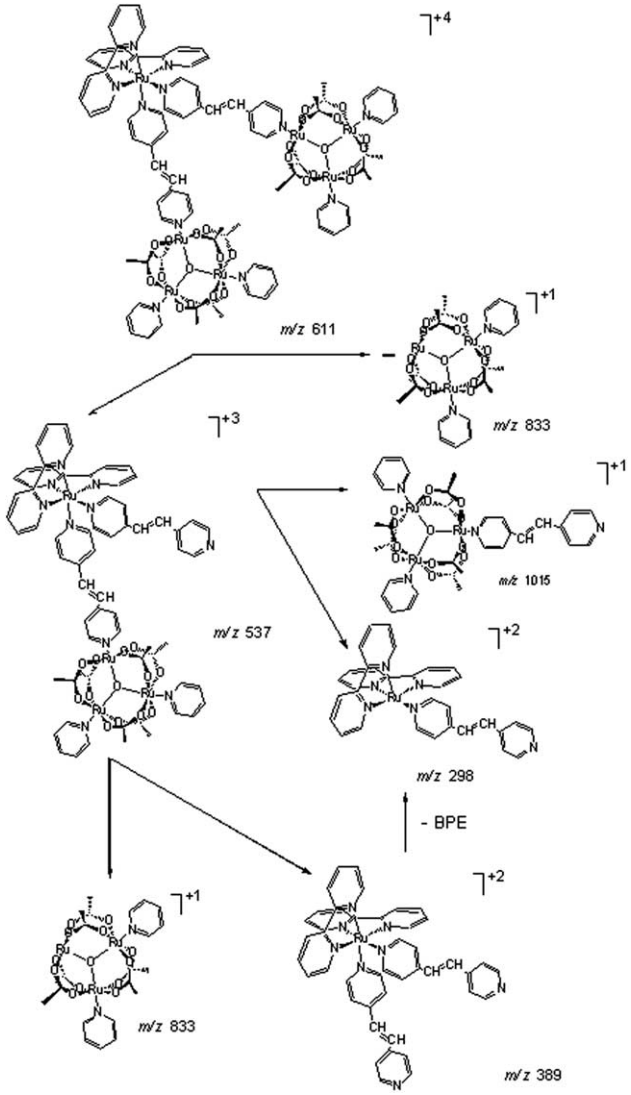

Fig. 3. Dissociation routes for the 15 eV collision-induced dissociation of gaseous [Ru(bpy)$_2$(BPE)$_2${Ru$_3$O(CH$_3$COO)$_6$(py)$_2$}$_2$]$^{4+}$ ions.

charged Ru_7-precursor ions (*m*/*z* 610) dissociate by charge partitioning, with BPE–Ru bond breaking, to form both a triply charged cluster of Ru_4-isotopologue fragment ions (*m*/*z* 537) separated by 1/3 *m*/*z* units and a singly charged cluster of Ru_3-isotopologue ions (*m*/*z* 833) separated by one *m*/*z* unit. The triply charged Ru_4-isotopologue ions (*m*/*z* 537) dissociate in turn via two competitive pathways that give either (i) a doubly charged cluster of Ru_1-isotopologue fragment ions (*m*/*z* 389) separated by 1/2 *m*/*z* units and a singly charged cluster of Ru_3-isotopologue fragment ions (*m*/*z* 833) or (ii) a singly charged cluster of Ru_3-isotopologue fragment ions (*m*/*z* 1015) and doubly charged cluster of Ru_1-isotopologue fragment ions (*m*/*z* 298) separated by 1/2 *m*/*z* units. These ions can also be formed from the doubly charged Ru_1-isotopologue fragment ions (*m*/*z* 389) via the loss of a neutral molecule of BPE. Note in Fig. 3, the characteristic isotopic distribution of both the Ru_7-precursor ion and of all of its Ru_n-fragment ions as well as the charge-diagnostic *m*/*z* separation within each cluster, matching perfectly those expected for the proposed structures.

3.3. Absorption spectra

In Fig. 4 one can see the absorption spectra of the $[Ru(bpy)_2(BPE)_2\{Ru_3O(CH_3COO)_6(py)_2\}_2](PF_6)_4$ complex. The spectra can be readily interpreted by comparing with the reported data for the model compounds $[Ru(bpy)_2(BPE)_2](PF_6)_2$ and $[Ru_3O(CH_3COO)_6(py)_2(BPE)]PF_6$ [33–35]. The intense bands in the ultra-violet region, i.e., 291 nm ($\varepsilon = 11.7 \times 10^4\ mol^{-1}\ l\ cm^{-1}$) can be assigned to the pyridinic ligand $\pi \rightarrow \pi^*$ transitions; in the visible region one can observe the MLCT bands of the $[Ru(bpy)_2]$ unit at 427 nm ($3.89 \times 10^4\ mol^{-1}\ l\ cm^{-1}$), as confirmed by spectroelectrochemical measurements. Finally, the near infra-red broad band at 696 nm ($1.29 \times 10^4\ mol^{-1}\ l\ cm^{-1}$) is consistent with the typical IC (intra-cluster) transitions, which occurs within an energy level manifold, generated by the combination of the ruthenium and central oxygen orbitals in the $[Ru_3O(CH_3COO)_6]$ fragment [35].

It is worth noting that the bridging coordination of the $[Ru_3O]$ cores does not affect significantly the energy of the MLCT bands, in comparison to the mononuclear precursors $[Ru(bpy)_2(BPE)_2]^{2+}$ ($\lambda_{max} = 430$ nm); the same is valid for the IC transition, in comparison with the $[Ru_3O(CH_3COO)_6(py)_2(BPE)]PF_6$ complex ($\lambda_{max} = 693$ nm) [33–35].

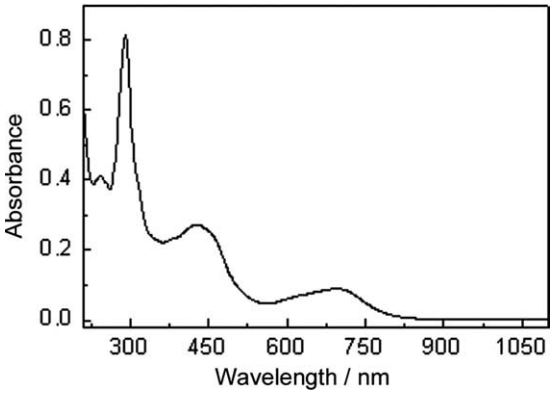

Fig. 4. Absorption spectrum of the $[Ru(bpy)_2(BPE)_2\{Ru_3O(CH_3COO)_6(py)_2\}_2](PF_6)_4$ complex, in acetonitrile solution.

3.4. Electrochemical measurements

The profile of the voltammograms shown in Fig. 5 consists of four reversible, two electron waves at −1.02, 0.16, 1.20, 2.11 V (versus SHE), ascribed to the $[Ru_3O]^{1-/0/1+/2+/3+}$ redox processes, one mono-electronic wave at 1.48 V, ascribed to the $Ru^{2+/3+}$ pair and finally a wave corresponding to the reduction of the pyridinic ligands. The peak current relation observed for the $[Ru_3O]^{1+/2+}$ and $Ru^{2+/3+}$ pairs have an approximated value of 2:1, being consistent with the proposed coordination of one $[Ru(bpy)_2]$ moiety to two $[Ru_3O]$ cores. The occurrence of only one wave associated with the redox processes in the two $[Ru_3O]$ units demonstrates that electronic coupling between them is not enough to promote detectable splittings in the cyclic voltammograms.

In Fig. 6 one can see the results of the spectroelectrochemical measurements. The observed behavior is consistent with that of monomeric trinuclear complexes [1], as well as with that of analogous polynuclear systems [36,37]. The first reduction process (Fig. 6(a)) implies in a destabilization of the $[Ru_3O]$ energy levels, owing to the increase of electron population, causing bathochromic shifts of both IC (696–915 nm) and

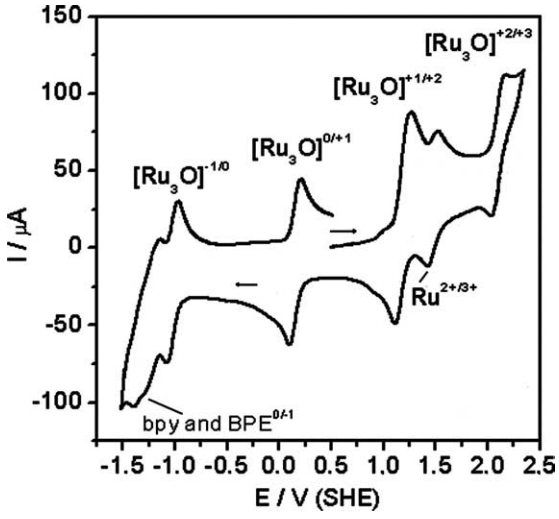

Fig. 5. Cyclic voltammogram of the $[Ru(bpy)_2(BPE)_2\{Ru_3O(CH_3COO)_6(py)_2\}_2](PF_6)_4$ complex in 3×10^{-3} mol l acetonitrile solutions, 0.1 mol l TEAP, room temperature, scan rate = 200 mV s^{-1}.

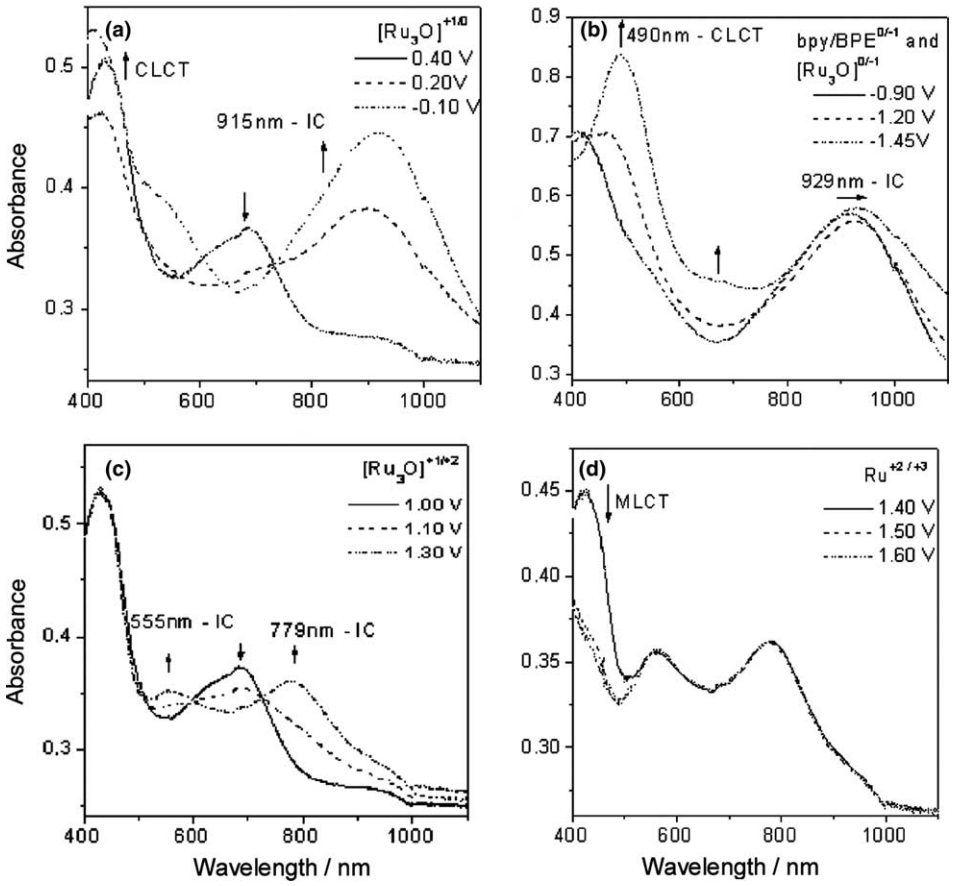

Fig. 6. Spectroelectrochemical behavior of $[Ru(bpy)_2(BPE)_2\{Ru_3O(CH_3COO)_6(py)_2\}_2](PF_6)_4$ in 3×10^{-3} mol l acetonitrile solutions, 0.1 mol l TEAP, as a function of the applied potentials.

CLCT bands (intensification of the shoulder observed between 400 and 500 nm). In the second reduction process (Fig. 6(b)), besides an additional destabilization of the $[Ru_3O]$ levels due to the addition of a second electron to each unit, an increase in intensity around 680 nm is observed, ascribed to a CLCT transition to the BPE bridge; this behavior is in agreement with that observed earlier for trinuclear complexes bridged by π-conjugated ligands [10,36,38].

The oxidation of the $[Ru_3O]$ center (Fig. 6(c)) is accompanied by the splitting of the IC band at 696 nm into two components at 555 and 779 nm. Finally, the oxidation of the $[Ru(bpy)_2]$ moiety, centered in the metal, leads to the decay of the MLCT band (Fig. 6(d)), once the electron involved in this transition is removed.

Under the experimental conditions of the spectroelectrochemical measurements, it was not possible to reach the positive potential corresponding to the last oxidation wave observed in the cyclic voltammetry.

3.5. Photophysical assays

Many attempts to detect luminescence emission for the complex were made in this work. In general, degassed solutions of the compound, in acetonitrile, ethanol (room temperature), and in ethanol glasses (77 K), were excited at the MLCT wavelength, but in no case the typical MLCT[3] luminescence of the $[Ru(bpy)_n]$ chromophore [13] could be detected. Also, the expected photoisomerization of the coordinated BPE ligand was not observed, in contrast to the free BPE ligand, which exhibited a *cis–trans* isomerization quantum yield of $\phi = 0.24$ in 10% acetonitrile:water solution, in agreement with the literature data [39].

For a series of $[Ru(bpy)_2(Cl)B]^{2+}$ compounds, in which B = pyrazine, 4-4′-bipyridine, 1,2-*bis*(4-pyridyl)ethane or *trans*-1,2-*bis*(4-pyridyl)ethylene (BPE), it has been observed that the emission quantum yield (ϕ_{em}) is extremely low, owing to d–d states [40]. Nevertheless, for the compound containing the bridging BPE ligand, the value of ϕ_{em} is even lower, indicating an additional pathway for energy loss, such as an energy transfer from the ^{3}MLCT to the BPE triplet state involved in photoisomerization. For the $[Ru(bpy)_2(BPE)_2\{Ru_3O(CH_3COO)_6(py)_2\}_2](PF_6)_4$ complex, this particular BPE excited state can undergo further energy (or electron) transfer to the $[Ru_3O]$ low lying IC states, which would finally decay by a non-radiative mechanism, thus, explaining the quenching of the *trans* → *cis*

photoisomerization. Actually, it has been shown that both energy and electron transfer can provide possible quenching pathways of ^{3}MCLT states (and probably of the bridge low lying triplet state), depending on the oxidation state of the $[Ru_3O]$ core [37].

4. Final remarks

A novel heptanuclear doubly bridged complex $[Ru(bpy)_2(BPE)_2\{Ru_3O(CH_3COO)_6(py)_2\}_2](PF_6)_4$ has been described. Detailed structural characterization of this supramolecular complex by ESI-MS(/MS) and NMR spectroscopy is fully consistent with the binding of two $[Ru_3O]$ units to the $[Ru(bpy)_2]$ center. The observed absorption profile, as well as its electrochemical behavior, are in agreement with a doubly bridged structure involving weakly interacting metallic units. Such weak electronic interaction, however, is strong enough to quench its photophysical properties, so that the emission from the $[Ru(bpy)_2]$ center has not been observed, either at room temperature or at 77 K, also preventing the characteristic *trans* → *cis* photoisomerization of the BPE bridging ligand.

Acknowledgments

We acknowledge the Brazilian agencies CNPq, CAPES and FAPESP and the Millennium Institute of Complex Materials.

References

[1] H.E. Toma, K. Araki, A.D.P. Alexiou, S. Nikolaou, S. Dovidauskas, Coord. Chem. Rev. 219 (2001) 187.
[2] A.D.P. Alexiou, S. Dovidauskas, H.E. Toma, Quim. Nova 23 (2000) 785.
[3] T.M. Busleva, S.N. Red'kina, O.V. Rudnitskaya, Russ. J. Coord. Chem. 25 (1999) 3.
[4] R.C. Rocha, H.E. Toma, Quim. Nova 25 (2002) 624.
[5] H.E. Toma, C.J. Cunha, C. Cipriano, Inorg. Chim. Acta 154 (1988) 63.
[6] A.D.P. Alexiou, H.E. Toma, J. Chem. Res. (S) (1993) 464.
[7] H.E. Toma, C. Cipriano, J. Electroanal. Chem. 263 (1989) 313.
[8] H.E. Toma, F. Matsumoto, C. Cipriano, J. Electroanal. Chem. 346 (1993) 261.
[9] S. Nikolaou, H.E. Toma, J. Chem. Res. (S) (2000) 326.
[10] (a) H.E. Toma, A.D.P. Alexiou, J. Braz. Chem. Soc. 6 (1995) 267; (b) H.E. Toma, A.D.P. Alexiou, J. Chem. Res. (S) (1995) 134.
[11] (a) K. Araki, S. Dovidauskas, H. Winnischofer, A.D.P. Alexiou, H.E. Toma, J. Electroanal. Chem. 498 (2001) 152; (b) S. Dovidauskas, K. Araki, H.E. Toma, J. Porphyr. Phthaloc. 4 (2000) 727; (c) S. Dovidauskas, H.E. Toma, K. Araki, H.C. Sacco, Y. Iamamoto, Inorg. Chim. Acta 305 (2000) 206; (d) H.E. Toma, K. Araki, E.O. Silva, Monatsh. Chem. 129 (1998) 975.
[12] T. Ito, T. Hamaguchi, H. Nagino, T. Yamaguchi, J. Washington, C.P. Kubbiak, Science 227 (1997) 660.
[13] A. Juris, V. Balzani, F. Barigelletti, S. Campagna, P. Belser, A. von Zelewsky, Coord. Chem. Rev. 84 (1988) 85.
[14] (a) V. Balzani, A. Juris, M. Venturi, S. Campagna, S. Serroni, Chem. Rev. 96 (1996) 759; (b) L. de Cola, P. Belser, Coord. Chem. Rev. 177 (1998) 301.
[15] (a) M. Venturi, A. Credi, V. Balzani, Coord. Chem. Rev. 185 (1999) 233; (b) F. Scandola, R. Argazzi, C.A. Bignozzi, M.T. Indelli, J. Photochem. Photobiol. A 82 (1994) 191; (c) F. Scandola, R. Argazzi, C.A. Bignozzi, C. Chiorboli, M.T. Indelli, M.A. Rampi, Coord. Chem. Rev. 125 (1993) 283.
[16] (a) V. Balzani, F. Scandola, in: Supramolecular Photochemistry, Ellis Horwood Chichester, UK, 1991; (b) R. Bergonzi, L. Fabbrizzi, M. Licchelli, C. Mangano, Coord. Chem. Rev. 170 (1998) 31; (c) S. Campagna, C. Di Pietro, F. Loiseau, B. Maubert, N. McClenaghan, R. Passalacqua, F. Puntoriero, V. Ricevuto, S. Serroni, Coord. Chem. Rev. 229 (2002) 67; (d) S. Serroni, S. Campagna, F. Puntoriero, C. Di Pietro, N.D. McClenaghan, F. Loiseau, Chem. Soc. Rev. 30 (2001) 367.
[17] H. Meier, Angew. Chem., Int. Ed. Engl. 31 (1992) 1399.
[18] H. Görner, F. Elisei, U. Mazzucato, J. Phys. Chem. 95 (1991) 4000.
[19] V.W. Yam, V.C. Lau, L. Wu, J. Chem. Soc., Dalton Trans. (1998) 1461.
[20] P. Gütlich, Y. Garcia, T. Woike, Coord. Chem. Rev. 219 (2001) 839.
[21] R. Ziessel, M. Hissler, A. El-ghayoury, A. Harriman, Coord. Chem. Rev. 178 (1998) 1251.
[22] V. Balzani, A. Credi, F.M. Raymo, J.F. Stoddart, Angew. Chem. Int. Ed. 39 (2000) 3348.
[23] (a) B.P. Sullivan, D.J. Salmon, T.J. Meyer, Inorg. Chem. 17 (1978) 3334; (b) S.A. Adeyemi, E.C. Johnson, F.J. Miller, T.J. Meyer, Inorg. Chem. 12 (1973) 2371; (c) M.J. Powers, T.J. Meyer, J. Am. Chem. Soc. 102 (1980) 1289.
[24] J.B. Domingos, E. Longhinotti, T.A.S. Brandão, L.S. Santos, M.N. Eberlin, C.A. Bunton, F. Nome, J. Org. Chem. 69 (2004) 7898.
[25] E.C. Constable, J. Lewis, Inorg. Chim. Acta 70 (1983) 251.
[26] S. Nikolaou, M. Uemi, H.E. Toma, Spectrosc. Lett. 34 (2001) 267.
[27] E.C. Constable, K.R.A. Seddon, J. Chem. Soc., Chem. Commun. (1982) 34.
[28] (a) S. Sun, E. Robson, N. Dunwoody, A.S. Silva, I.M. Brinn, A.J. Lees, Chem. Commun. (2000) 201; (b) V.W. Yam, V.C. Lau, L. Wu, J. Chem. Soc., Dalton Trans. (1998) 1461.
[29] I. Bertini, C. Luchinat, Coord. Chem. Rev. 150 (1996) 1.
[30] Standard Spectra Collection, Sadtler Research Lab., Bio-Rad Inc., Philadelphia, PA.
[31] (a) R. Colton, A. D'Agostinho, J.C. Traeger, Mass Spectrom. Rev. 14 (1995) 79; (b) D.A. Plattner, Int. J. Mass Spectrom. 207 (2001) 125; (c) J. Griep-Raming, S. Meyer, T. Bruhn, J.O. Metzger, Angew. Chem. Ind. Ed. 41 (2002) 2738; (d) R. Arakawa, S. Tachiyashiki, T. Matsuo, Anal. Chem. 67 (1995) 4133.
[32] (a) D.M. Tomazela, I. Mayer, F.M. Engelmann, K. Araki, H.E. Toma, M.N. Eberlin, J. Mass Spectrom. 39 (2004) 1161; (b) S.H. Toma, M. Uemi, S. Nikolaou, D.M. Tomazela, M.N. Eberlin, H.E. Toma, Inorg. Chem. 43 (2004) 3521; (c) D.M. Tomazela, F.C. Gozzo, G. Eberling, J. Dupont, M.N. Eberlin, Inorg. Chim. Acta 357 (2004) 2349; (d) R.M.S Pereira, V.I. Paula, R. Buffon, D.M. Tomazela, M.N. Eberlin, Inorg. Chim. Acta 357 (2004) 2100; (e) G. Cerchiaro, P.L. Saboya, A.M. da Costa Ferreira, D.M. Tomazela, M.N. Eberlin, Trans. Metal Chem. 29 (2004) 495;

(f) S.H. Toma, S. Nikolaou, D.M. Tomazela, M.N. Eberlin, H.E. Toma, Inorg. Chim. Acta 357 (2004) 2253;
(g) A.A. Sabino, A.H.L. Machado, C.R.D. Correia, M.N. Eberlin, Angew. Chem. Int. Ed. 43 (2004) 2514.
[33] R.W. Callahan, G.M. Brown, T.J. Meyer, Inorg. Chem. 14 (1975) 1443.
[34] M.J. Powers, R.W. Callahan, D.J. Salmon, T.J. Meyer, Inorg. Chem. 15 (1976) 894.
[35] J.A. Baumann, D.J. Salmon, S.T. Wilson, T.J. Meyer, W.E. Hatfield, Inorg. Chem. 17 (1978) 3342.
[36] S. Nikolaou, H.E. Toma, Polyhedron 20 (2001) 253.
[37] S. Nikolaou, H.E. Toma, J. Chem. Soc., Dalton Trans. (2002) 352.
[38] (a) J.A. Baumann, D.J. Salmon, S.T. Wilson, T.J. Meyer, Inorg. Chem. 18 (1979) 2472;
(b) J.A. Baumann, S.T. Wilson, D.J. Salmon, P.L. Hood, T.J. Meyer, J. Am. Chem. Soc. 101 (1979) 2916;
(c) S.T. Wilson, R.F. Bondurant, T.J. Meyer, D.J. Salmon, J. Am. Chem. Soc. 97 (1975) 2285.
[39] (a) D.G. Whitten, M.T. McCall, Tetrahedron Lett. 23 (1968) 2755;
(b) D.G. Whitten, M.T. McCall, J. Am. Chem. Soc. 91 (1969) 5097;
(c) D.G. Whitten, Y.J. Lee, J. Am. Chem. Soc. 92 (1970) 415;
(d) Y.J. Lee, D.G. Whitten, L. Pedersen, J. Am. Chem. Soc. 93 (1971) 6330;
(e) D.G. Whitten, Y.J. Lee, J. Am. Chem. Soc. 94 (1972) 9142;
(f) A.R. Gutierrez, D.G. Whitten, J. Am. Chem. Soc. 98 (1976) 6233.
[40] J.C. Curtis, J.S. Berstein, T.J. Meyer, Inorg. Chem. 24 (1985) 385.